Eur. Phys. J. C 28, 365–374 (2003)
Digital Object Identifier (DOI) 10.1140/epjc/s2003-01184-6

THE EUROPEAN PHYSICAL JOURNAL C

Probing the Majorana mass scale of right-handed neutrinos in mSUGRA

F. Deppisch[1,a], H. Päs[1,b], A. Redelbach[1,c], R. Rückl[1,d], Y. Shimizu[2,e]

[1] Institut für Theoretische Physik und Astrophysik, Universität Würzburg, 97074 Würzburg, Germany
[2] Department of Physics, Nagoya University, Nagoya 464-8602, Japan

Received: 14 June 2002 / Revised version: 7 January 2003 /
Published online: 14 April 2003 –

Abstract. We discuss the perspectives of testing the right-handed Majorana mass scale $M_{\rm R}$ of the SUSY see-saw model in the mSUGRA framework. Lepton-flavor violating low energy processes are analyzed in recently proposed post-LEP benchmark scenarios, taking into account present uncertainties and future developments in the neutrino sector. Non-observation of $\mu \to e\gamma$ in the next-generation PSI experiment will provide upper bounds on $M_{\rm R}$ of the order of $10^{12\div 14}$ GeV, while on the other hand, a positive signal for $\tau \to \mu\gamma$ at SUPERKEKB or the LHC may determine $M_{\rm R}$ for a given mSUGRA scenario with an accuracy of a factor of 2.

1 Introduction

With the evidence for neutrino masses and mixing in solar [1] and atmospheric [2] neutrino experiments, studies of the lepton sector have gained importance as a path to physics beyond the standard model. The most elegant and widely accepted explanation for small neutrino masses is provided by the see-saw mechanism [3], in which a large Majorana mass scale $M_{\rm R}$ of right-handed neutrinos drives the light neutrino masses down to or below the sub-eV scale, as required by the experimental evidence. A priori, the fundamental scale $M_{\rm R}$ can be of the order of the GUT scale and may thus be unaccessible for any kind of direct experimental tests. However, neutrino mixing implies lepton-flavor violation (LFV), which is absent in the standard model and provides indirect probes of $M_{\rm R}$. While lepton-flavor violating processes are suppressed due to the small neutrino masses if only right-handed neutrinos are added to the standard model [4], in supersymmetric models new sources of LFV exist. For example, virtual effects of the massive neutrinos affect the renormalization group equations (RGEs) of the slepton mass and the trilinear coupling matrices and give rise to non-diagonal terms inducing LFV.

Assuming the experimentally favored large mixing angle (LMA) MSW solution of the solar neutrino anomaly, one can expect lepton-flavor violating μ and τ decays with branching ratios close to the current experimental bounds [5]. Some of the existing bounds will be improved significantly in the near future. The current experimental limits (future sensitivities) on low-energy lepton-flavor violating processes involving charged leptons can be summarized as follows:

$$\begin{aligned}
&{\rm Br}(\mu \to e\gamma) < 1.2 \cdot 10^{-11} (10^{-14}) \quad [6,7],\\
&{\rm Br}(\tau \to e\gamma) < 2.7 \cdot 10^{-6} \quad [8],\\
&{\rm Br}(\tau \to \mu\gamma) < 1.1 \cdot 10^{-6} (10^{-9}) \quad [9,10],\\
&{\rm Br}(\mu^+ \to e^+e^+e^-) < 1.0 \cdot 10^{-12} \quad [11],\\
&R(\mu^-{\rm Ti} \to e^-{\rm Ti}) < 6.1 \cdot 10^{-13} (10^{-14}) \quad [12,13].
\end{aligned} \tag{1}$$

Here, the observable R denotes the cross-section normalized to the total muon capture rate. The MECO experiment aims at a sensitivity for $\mu^-{\rm Al} \to e^-{\rm Al}$ below $R \approx 10^{-16}$ [14]. In the farther future, the PRISM project plans to provide beams of low-energy muons with an intensity increased by several orders of magnitude, so that it may become possible to reach ${\rm Br}\,(\mu \to e\gamma) \approx 10^{-15}$ [15], ${\rm Br}\,(\mu^+ \to e^+e^+e^-) \approx 10^{-16}$ [16] and $R\,(\mu^-{\rm Ti} \to e^-{\rm Ti}) \approx 10^{-18}$ [17] (see also the review of [18]). Searches for $\tau \to \mu\gamma$ at the LHC or SUPERKEKB are expected to probe LFV in this channel at the level of ${\rm Br} \approx 10^{-9}$ [10].

The above processes in the context of supersymmetric see-saw models have been considered in several previous studies (see e.g. [5,19–24]). In [19] it has been pointed out that the corresponding branching ratios and cross-sections exhibit a quadratic dependence on the right-handed Majorana neutrino mass scale $M_{\rm R}$. Therefore, the exploration of these processes provides very interesting possibilities to constrain $M_{\rm R}$. In the present paper, we sharpen the current knowledge of these constraints by investigating in more detail which information about the right-handed Majorana masses can be extracted from measurements

[a] e-mail: deppisch@physik.uni-wuerzburg.de
[b] e-mail: paes@physik.uni-wuerzburg.de
[c] e-mail: asredelb@physik.uni-wuerzburg.de
[d] e-mail: rueckl@physik.uni-wuerzburg.de
[e] e-mail: shimizu@eken.phys.nagoya-u.ac.jp

of the processes (1). It is assumed that the right-handed Majorana masses are degenerate at the scale $M_{\rm R}$. We focus on the recently proposed post-LEP mSUGRA benchmark scenarios [25], and take into account the uncertainties in the neutrino parameters. In addition, we show by how much the sensitivity to $M_{\rm R}$ will improve with future more precise neutrino data. Our work updates and extends previous studies in several directions. Firstly, the mSUGRA scenarios of [25] have been developed particularly for linear collider studies but have not yet been applied to lepton-flavor violating processes at low energies. Our study clarifies the model-dependence of the latter for this very relevant set of mSUGRA models. Secondly, the neutrino input in our analysis is varied in the ranges allowed by present data. The results are compared to expectations for more precise neutrino measurements in the future. Thirdly, we consider degenerate as well as hierarchical neutrino spectra, and study the impact a future determination of the absolute neutrino mass scale would make. Finally, following [26] it is demonstrated that the influence of the mSUGRA scenarios in the tests of $M_{\rm R}$ can be reduced by normalizing $\mathrm{Br}(l_i \to l_j\gamma)$ to the corresponding SUSY contribution to the muon anomalous magnetic moment.

This paper is organized as follows. In Sect. 2, we discuss the supersymmetric see-saw mechanism and the renormalization group evolution of the neutrino and slepton mass matrices. In Sect. 3, the rare decays $l_i \to l_j\gamma$, $\mu \to 3e$ as well as μ–e conversion in nuclei are briefly reviewed, and the most important results for our investigations are displayed. Also the anomalous magnetic moment of the muon and the correlation with $l_i \to l_j\gamma$ is discussed there. Section 4 summarizes the input parameters of the mSUGRA benchmark scenarios and the experimental neutrino data used in the analysis. The numerical results of our studies are presented in Sect. 5, and conclusions are drawn in Sect. 6.

2 Supersymmetric see-saw mechanism

The supersymmetric see-saw mechanism is described by the term [20]

$$W_\nu = -\frac{1}{2}\nu_{\rm R}^{\rm cT} M \nu_{\rm R}^{\rm c} + \nu_{\rm R}^{\rm cT} Y_\nu L \cdot H_2 \tag{2}$$

in the superpotential, where $\nu_{{\rm R}a}$ ($a = e, \mu, \tau$) are the right-handed neutrino singlet fields, L_a denote the left-handed lepton doublets and H_2 is the Higgs doublet with hypercharge $+\frac{1}{2}$. The 3×3 matrix M is the Majorana mass matrix, while Y_ν is the matrix of neutrino Yukawa couplings leading to the Dirac mass matrix $m_{\rm D} = Y_\nu \langle H_2^0 \rangle$, $\langle H_2^0 \rangle = v \sin\beta$ being the H_2 vacuum expectation value with $v = 174\,\mathrm{GeV}$ and $\tan\beta = \frac{\langle H_2^0 \rangle}{\langle H_1^0 \rangle}$. Light neutrinos can be naturally explained if one assumes that the Majorana scale $M_{\rm R}$ of the mass matrix M is much larger than the scale of the Dirac mass matrix $m_{\rm D}$, which is of the order of the electroweak scale. At energies much smaller than $M_{\rm R}$ one has an effective superpotential with

$$W_\nu^{\rm eff} = \frac{1}{2}(Y_\nu L \cdot H_2)^{\rm T} M^{-1} (Y_\nu L \cdot H_2). \tag{3}$$

The corresponding mass term for the left-handed neutrinos $\nu_{{\rm L}a}$ is then given by

$$-\frac{1}{2}\nu_{\rm L}^{\rm T} M_\nu \nu_{\rm L} + \mathrm{h.c.}, \tag{4}$$

where the mass matrix

$$M_\nu = m_{\rm D}^{\rm T} M^{-1} m_{\rm D} = Y_\nu^{\rm T} M^{-1} Y_\nu (v \sin\beta)^2 \tag{5}$$

is suppressed by the large Majorana scale $M_{\rm R}$. In the following we work in the basis where the charged lepton Yukawa coupling matrix Y_l [1] and the Majorana mass matrix M of the right-handed neutrinos are diagonal, which is always possible. The matrix M_ν is diagonalized by the unitary MNS matrix U,

$$U^{\rm T} M_\nu U = \mathrm{diag}(m_1, m_2, m_3), \tag{6}$$

that relates the neutrino flavor and mass eigenstates:

$$\begin{pmatrix} \nu_e \\ \nu_\mu \\ \nu_\tau \end{pmatrix} = U \begin{pmatrix} \nu_1 \\ \nu_2 \\ \nu_3 \end{pmatrix}. \tag{7}$$

In general, U can be written in the form

$$U = V \cdot \mathrm{diag}(\mathrm{e}^{\mathrm{i}\phi_1}, \mathrm{e}^{\mathrm{i}\phi_2}, 1), \tag{8}$$

where ϕ_1, ϕ_2 are Majorana phases and V can be parametrized in the standard CKM form:

$$V = \begin{pmatrix} c_{13}c_{12} & c_{13}s_{12} & s_{13}\mathrm{e}^{-\mathrm{i}\varphi} \\ -c_{23}s_{12} - s_{23}s_{13}c_{12}\mathrm{e}^{\mathrm{i}\varphi} & c_{23}c_{12} - s_{23}s_{13}s_{12}\mathrm{e}^{\mathrm{i}\varphi} & s_{23}c_{13} \\ s_{23}s_{12} - c_{23}s_{13}c_{12}\mathrm{e}^{\mathrm{i}\varphi} & -s_{23}c_{12} - c_{23}s_{13}s_{12}\mathrm{e}^{\mathrm{i}\varphi} & c_{23}c_{13} \end{pmatrix}. \tag{9}$$

The experimental data on neutrino oscillations determine or at least constrain the mixing matrix V and the differences of the squared mass eigenvalues m_i at a scale not far from the electroweak scale. We will therefore identify these two scales in our analysis. Using the results of recent neutrino fits and making some further necessary assumptions on the neutrino spectrum one can reconstruct $M_\nu(M_Z)$ from (6).

2.1 Renormalization group evolution of the neutrino sector

In order to calculate the lepton-flavor violating contributions to the slepton mass matrix in a top-down approach from the unification scale $M_X \approx 2 \cdot 10^{16}\,\mathrm{GeV}$ to the electroweak scale, we first need to evolve the neutrino mass

[1] Therefore, we do not have to discriminate flavor and mass eigenstates for charged leptons, i.e. $l_{e,\mu,\tau} = l_{1,2,3} = e, \mu, \tau$

matrix $M_\nu(M_Z)$ to M_X. Below $M_{\rm R}$, the one-loop RGE in the MSSM is given by [27]

$$\frac{\mathrm{d}}{\mathrm{d}t}M_\nu = \frac{1}{16\pi^2}\left(\left(-6g_2^2-\frac{6}{5}g_1^2+\mathrm{Tr}(6Y_U^\dagger Y_U)\right)M_\nu + \left((Y_l^\dagger Y_l)M_\nu + M_\nu(Y_l^\dagger Y_l)^{\mathrm{T}}\right)\right), \quad (10)$$

with the U(1) and SU(2) gauge couplings g_1 and g_2, and the Yukawa coupling matrices Y_U and Y_l for the charge $\frac{2}{3}$-quarks and charged leptons, respectively. The corresponding evolution equations for $g_{1,2}$, Y_U and Y_l can be found in [28]. The RGE is linear in M_ν and can thus be solved analytically [27]:

$$M_\nu(t) = I(t)\cdot M_\nu(0)\cdot I(t), \quad t=\ln\left(\frac{\mu}{M_Z}\right). \quad (11)$$

Since the evolution is dominated by the gauge and third generation Yukawa couplings one obtains, to a good approximation:

$$I(t) = I_g I_t\,\mathrm{diag}\,(1,1,I_\tau), \quad (12)$$

with

$$I_g(t) = \exp\left(\frac{1}{16\pi^2}\int_0^t\left(-3g_2^2-\frac{3}{5}g_1^2\right)\mathrm{d}t'\right), \quad (13)$$

$$I_t(t) = \exp\left(\frac{1}{16\pi^2}\int_0^t 3|Y_t|^2\mathrm{d}t'\right), \quad (14)$$

$$I_\tau(t) = \exp\left(\frac{1}{16\pi^2}\int_0^t |Y_\tau|^2\mathrm{d}t'\right). \quad (15)$$

To calculate these factors, the MSSM RGEs for the gauge and Yukawa couplings are solved in one-loop approximation, neglecting threshold effects.

In order to proceed with the evolution from $M_{\rm R}$ to M_X we use directly the matrix Y_ν of the neutrino Yukawa couplings. From (5) and (6) one finds [20]

$$Y_\nu = \frac{1}{v\sin\beta}\mathrm{diag}(\sqrt{M_1},\sqrt{M_2},\sqrt{M_3})\cdot R \cdot\mathrm{diag}(\sqrt{m_1},\sqrt{m_2},\sqrt{m_3})\cdot U^\dagger, \quad (16)$$

where M_i are the Majorana masses of the right-handed neutrinos and R is an unknown orthogonal matrix. As we will see, the lepton-flavor violating terms in the slepton mass matrix depend on Y_ν only through the combination $Y_\nu^\dagger Y_\nu$. In this work, we assume the right-handed Majorana masses to be degenerate at $M_{\rm R}$ ($M_1=M_2=M_3=M_{\rm R}$) and the matrix R to be real. Then the product $Y_\nu^\dagger Y_\nu$ simplifies to

$$Y_\nu^\dagger Y_\nu = \frac{M_{\rm R}}{v^2\sin^2\beta}U\cdot\mathrm{diag}(m_1,m_2,m_3)\cdot U^\dagger, \quad (17)$$

thus being independent of R. Therefore this class of models is highly predictive and is often used for phenomenological studies. In addition, one obtains more conservative upper bounds on $M_{\rm R}$ for real R because a complex matrix R generically leads to larger values of $Y_\nu^\dagger Y_\nu$ and thus to larger branching ratios $\mathrm{Br}(l_i\to l_j\gamma)$ as shown in [20]. Furthermore, since the Majorana phases ϕ_1 and ϕ_2 defined in (8) also drop out in (17), U can be replaced by V in (16). Finally, the neutrino masses m_i and V are evaluated from M_ν at $M_{\rm R}$ using (6). The resulting matrix $Y_\nu(M_{\rm R})$ is then evolved from $M_{\rm R}$ to M_X using the one-loop RGE [20]

$$\frac{\mathrm{d}}{\mathrm{d}t}Y_\nu = \frac{1}{16\pi^2}Y_\nu\left(\left(-3g_2^2-\frac{3}{5}g_1^2+\mathrm{Tr}(3Y_U^\dagger Y_U+Y_\nu^\dagger Y_\nu)\right)\mathbf{1} + Y_l^\dagger Y_l + 3Y_\nu^\dagger Y_\nu\right), \quad (18)$$

and keeping the product $Y_\nu^\dagger Y_\nu$ on the r.h.s. of (18) fixed at $M_{\rm R}$. The running of the right-handed mass matrix M between $M_{\rm R}$ and M_X is negligible, as we have checked numerically.

2.2 Renormalization group evolution of the slepton sector

Having evolved the neutrino Yukawa couplings or, more specifically, the product $Y_\nu^\dagger Y_\nu$, to the unification scale M_X, one can now run the slepton mass matrix from M_X to the electroweak scale assuming the mSUGRA universality conditions at M_X:

$$m_{\rm L}^2 = m_0^2\mathbf{1}, \qquad m_R^2 = m_0^2\mathbf{1}, \qquad A = A_0 Y_l, \quad (19)$$

where m_0 is the common scalar mass and A_0 is the common trilinear coupling. For the present analysis, we adopt the mSUGRA benchmark scenarios proposed recently in [25] for linear collider studies. The charged slepton (mass)^2 matrix has the form:

$$m_{\tilde l}^2 = \begin{pmatrix} m_{\tilde l_{\rm L}}^2 & (m_{\tilde l_{\rm LR}}^2)^\dagger \\ m_{\tilde l_{\rm LR}}^2 & m_{\tilde l_{\rm R}}^2\end{pmatrix}, \quad (20)$$

where $m_{\tilde l_{\rm L}}^2$, $m_{\tilde l_{\rm R}}^2$ and $m_{\tilde l_{\rm LR}}^2$ are 3×3 matrices, $m_{\tilde l_{\rm L}}^2$ and $m_{\tilde l_{\rm R}}^2$ being hermitian. The matrix elements are given by

$$(m_{\tilde l_{\rm L}}^2)_{ab} = (m_{\rm L}^2)_{ab} + \delta_{ab}\left(m_{l_a}^2 + m_Z^2\cos(2\beta)\left(-\frac{1}{2}+\sin^2\theta_{\rm W}\right)\right) \quad (21)$$

$$(m_{\tilde l_{\rm R}}^2)_{ab} = (m_{\rm R}^2)_{ab} + \delta_{ab}(m_{l_a}^2 - m_Z^2\cos(2\beta)\sin^2\theta_{\rm W}), \quad (22)$$

$$(m_{\tilde l_{\rm LR}}^2)_{ab} = A_{ab}v\cos\beta - \delta_{ab}m_{l_a}\mu\tan\beta, \quad (23)$$

$\theta_{\rm W}$ being the Weinberg angle and μ the SUSY Higgs- mixing parameter. After evolution from M_X to M_Z, one has

$$m_{\rm L}^2 = m_0^2\mathbf{1} + (\delta m_{\rm L}^2)_{\rm MSSM} + \delta m_{\rm L}^2, \quad (24)$$

$$m_{\rm R}^2 = m_0^2\mathbf{1} + (\delta m_{\rm R}^2)_{\rm MSSM} + \delta m_{\rm R}^2, \quad (25)$$

$$A = A_0 Y_l + \delta A_{\rm MSSM} + \delta A, \quad (26)$$

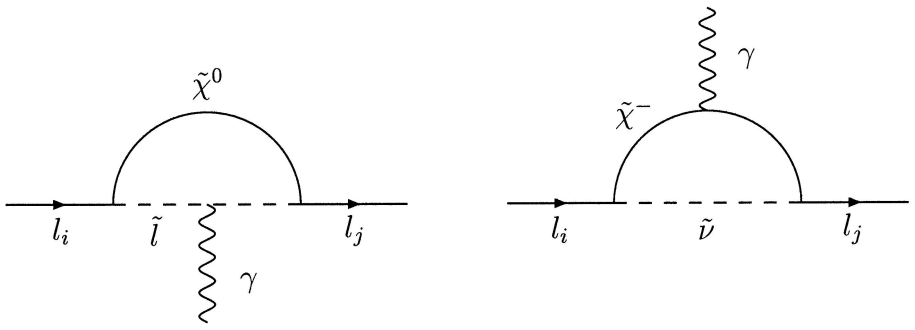

Fig. 1. Diagrams for $l_i^- \to l_j^- \gamma$ in the MSSM

where $(\delta m^2_{\mathrm{L,R}})_{\mathrm{MSSM}}$ and $(\delta A)_{\mathrm{MSSM}}$ denote the usual MSSM renormalization-group corrections [28] which are flavor-diagonal. In addition, the presence of right-handed neutrinos radiatively induces flavor off-diagonal terms denoted by $\delta m^2_{\mathrm{L,R}}$ and δA in (24) to (26). These corrections are taken into account in the approximation [19]

$$\delta m^2_{\mathrm{L}} = -\frac{1}{8\pi^2}(3m_0^2 + A_0^2)(Y_\nu^\dagger Y_\nu)\ln\left(\frac{M_X}{M_{\mathrm{R}}}\right), \quad (27)$$

$$\delta m^2_{\mathrm{R}} = 0, \quad (28)$$

$$\delta A = -\frac{3A_0}{16\pi^2}(Y_l Y_\nu^\dagger Y_\nu)\ln\left(\frac{M_X}{M_{\mathrm{R}}}\right). \quad (29)$$

It is these terms which give rise to lepton-flavor violating processes such as $l_i \to l_j\gamma$ and μ–e conversion.

The physical charged slepton masses are then found by diagonalizing (20) using the 6×6 unitary matrix $U_{\tilde{l}}$:

$$U_{\tilde{l}}^\dagger m_{\tilde{l}}^2 U_{\tilde{l}} = \mathrm{diag}(m^2_{\tilde{l}_1}, ..., m^2_{\tilde{l}_i}, ..., m^2_{\tilde{l}_6}). \quad (30)$$

Correspondingly, the slepton mass eigenstates are expressed in terms of the gauge eigenstates by

$$\tilde{l}_i = (U^*_{\tilde{l}})_{ai}\tilde{l}_{\mathrm{L}a} + (U^*_{\tilde{l}})_{(a+3)i}\tilde{l}_{\mathrm{R}a}, \qquad i = 1, ..., 6;\ a = e, \mu, \tau. \quad (31)$$

Similarly to (21), the 3×3 (mass)^2 matrix of the SUSY partners of the left-handed neutrinos is given by

$$(m^2_{\tilde{\nu}})_{ab} = (m^2_{\mathrm{L}})_{ab} + \frac{1}{2}\delta_{ab} m_Z^2 \cos(2\beta), \quad (32)$$

where m^2_{L} can be taken from (24). The partners of the right-handed neutrinos are very heavy and can therefore be disregarded. After diagonalization with the unitary 3×3 matrix $U_{\tilde{\nu}}$,

$$U_{\tilde{\nu}}^\dagger m^2_{\tilde{\nu}} U_{\tilde{\nu}} = \mathrm{diag}(m^2_{\tilde{\nu}_1}, m^2_{\tilde{\nu}_2}, m^2_{\tilde{\nu}_3}), \quad (33)$$

the mass eigenstates $\tilde{\nu}_i$ are related to the gauge eigenstates by

$$\begin{pmatrix} \tilde{\nu}_e \\ \tilde{\nu}_\mu \\ \tilde{\nu}_\tau \end{pmatrix} = U_{\tilde{\nu}} \begin{pmatrix} \tilde{\nu}_1 \\ \tilde{\nu}_2 \\ \tilde{\nu}_3 \end{pmatrix}. \quad (34)$$

3 LFV low-energy processes and $g_\mu - 2$

3.1 The radiative decays $l_i \to l_j\gamma$

The effective Lagrangian for $l_i^- \to l_j^-\gamma$ is given by [26]

$$\mathcal{L}_{\mathrm{eff}} = \frac{e}{2}\bar{l}_j \sigma_{\alpha\beta} F^{\alpha\beta}\left(A^{ij}_{\mathrm{L}} P_{\mathrm{L}} + A^{ij}_{\mathrm{R}} P_{\mathrm{R}}\right) l_i, \quad (35)$$

where $F^{\alpha\beta}$ is the electromagnetic field strength tensor, $\sigma_{\alpha\beta} = \frac{\mathrm{i}}{2}[\gamma_\alpha, \gamma_\beta]$ and $P_{\mathrm{R,L}} = \frac{1}{2}(1 \pm \gamma_5)$ are the helicity projection operators. The coefficients $A^{ij}_{\mathrm{L,R}}$ are determined by the photon penguin diagrams shown in Fig. 1 with charginos/sneutrinos or neutralinos/charged sleptons in the loop.

From (35) one obtains the following decay rate for $l_i^- \to l_j^-\gamma$ [5]:

$$\Gamma\left(l_i^- \to l_j^-\gamma\right) = \frac{\alpha}{4} m^3_{l_i}\left(|A^c_{\mathrm{L}} + A^n_{\mathrm{L}}|^2 + |A^c_{\mathrm{R}} + A^n_{\mathrm{R}}|^2\right). \quad (36)$$

The superscript $c\,(n)$ refers to the chargino (neutralino) diagram of Fig. 1, while the flavor indices are omitted. Because $m_{l_i} \gg m_{l_j}$ and $m^2_{\tilde{l}_{\mathrm{R}}}$ is diagonal (see (22), (25) and (28)), one has $A_{\mathrm{R}} \gg A_{\mathrm{L}}$ [19,20]. The dominant amplitudes in (36) are approximately given by

$$\begin{aligned} A^c_{\mathrm{R}} \simeq\ & \frac{1}{32\pi^2}\frac{g_2^2 m_{l_i}}{\sqrt{2} m_W \cos\beta} \\ & \times \sum_{a=1}^{2}\sum_{k=1}^{3} \frac{m_{\tilde{\chi}^-_a}}{m^2_{\tilde{\nu}_k}} (O_{\mathrm{R}})_{a1} (O_{\mathrm{L}})_{a2} (U^*_{\tilde{\nu}})_{jk} (U_{\tilde{\nu}})_{ik} \\ & \times \frac{1}{(1 - r^c_{ak})^3}\left(-3 + 4r^c_{ak} - (r^c_{ak})^2 - 2\ln r^c_{ak}\right), \quad (37) \\ A^n_{\mathrm{R}} \simeq\ & -\frac{1}{32\pi^2} g_2^2 \tan\theta_{\mathrm{W}} \\ & \times \sum_{a=1}^{4}\sum_{k=1}^{6} \frac{m_{\tilde{\chi}^0_a}}{m^2_{\tilde{l}_k}} (O_N)_{a1} \left((O_N)_{a2} + (O_N)_{a1}\tan\theta_{\mathrm{W}}\right) \\ & \times (U^*_{\tilde{l}})_{jk} (U_{\tilde{l}})_{(i+3)k} \frac{1}{(1 - r^n_{ak})^3} \\ & \times \left(1 - (r^n_{ak})^2 + 2r^n_{ak}\ln r^n_{ak}\right), \quad (38) \end{aligned}$$

with

$$r^c_{ak} = \left(\frac{m_{\tilde{\chi}^-_a}}{m_{\tilde{\nu}_k}}\right)^2, \qquad r^n_{ak} = \left(\frac{m_{\tilde{\chi}^0_a}}{m_{\tilde{l}_k}}\right)^2, \quad (39)$$

the chargino diagonalization matrices $O_{\rm L}, O_{\rm R}$ and the neutralino diagonalization matrix O_N. The mass eigenvalues of the charginos and neutralinos are denoted by $m_{\tilde{\chi}_a^-}$ and $m_{\tilde{\chi}_a^0}$, respectively. The numerical calculations discussed later are performed with the full expressions for $A_{\rm L}^{c,n}$ and $A_{\rm R}^{c,n}$, which can be found in [5,30].

Note that there is no difference between the rates of $l_i^- \to l_j^-\gamma$ and $l_i^+ \to l_j^+\gamma$ at the one-loop level and no CP violating observables can be constructed at this level of perturbation theory [30,31]. We therefore do not distinguish between $\mathrm{Br}(l_i^- \to l_j^-\gamma)$ and $\mathrm{Br}(l_i^+ \to l_j^+\gamma)$ in the following.

3.2 Br $(\mu \to 3e)$ and $R\,(\mu^- N \to e^- N)$

The processes $\mu \to 3e$ and $\mu^- N \to e^- N$ are dominated by photon penguin contributions. As a consequence, one has the following model-independent relations [19]:

$$\frac{\mathrm{Br}(\mu \to 3e)}{\mathrm{Br}(\mu \to e\gamma)} \approx \frac{\alpha}{8\pi}\frac{8}{3}\left(\ln\frac{m_\mu^2}{m_e^2} - \frac{11}{4}\right) \approx 7 \cdot 10^{-3}, \quad (40)$$

$$\frac{R(\mu^- N \to e^- N)}{\mathrm{Br}(\mu \to e\gamma)} \approx \frac{\Gamma_\mu}{\Gamma_{\rm cap}} 16\alpha^4 Z_{\rm eff}^4 Z |F(q^2)|^2 \quad (41)$$

$$\approx 6 \cdot 10^{-3} \qquad \text{for titanium}, \quad (42)$$

where Γ_μ is the total decay width of the muon, $F(q^2)$ is the nuclear form factor and Z ($Z_{\rm eff}$) is the electric (effective) charge of the nucleus. From the above and (1) one can see that the present experimental upper limits on $\mathrm{Br}\,(\mu \to 3e)$ and $R\,(\mu^- N \to e^- N)$ constrain LFV considerably less than the current limit on $\mathrm{Br}\,(\mu \to e\gamma)$. However, a future measurement of R in the range of $R\,(\mu^-\mathrm{Ti} \to e^-\mathrm{Ti}) \approx 10^{-18}$ [17] as mentioned in the introduction would provide a more sensitive test than the corresponding future sensitivity $\mathrm{Br}\,(\mu \to e\gamma) \approx 10^{-15}$.

We have examined the relations (40) to (42) numerically for the neutrino parameters and mSUGRA scenarios presented in the next section using complete analytic expressions [5], and we have found

$$\frac{\mathrm{Br}(\mu \to 3e)}{\mathrm{Br}(\mu \to e\gamma)} \approx (6-7) \cdot 10^{-3}, \quad (43)$$

$$\frac{R(\mu^-\mathrm{Ti} \to e^-\mathrm{Ti})}{\mathrm{Br}(\mu \to e\gamma)} \approx (5-7) \cdot 10^{-3}, \quad (44)$$

in good agreement with the above estimates.

3.3 Anomalous magnetic moment of the muon

The supersymmetric contribution to $\frac{1}{2}(g_\mu - 2)$ is described by the diagrams of Fig. 1 for $i = j = 2$. In this case the effective Lagrangian (35) yields [26]

$$\delta a_\mu = \frac{m_\mu}{2}\left(A_{\rm R}^{22} + A_{\rm L}^{22}\right), \quad (45)$$

Table 1. Input parameters of the mSUGRA benchmark scenarios and the predicted shift δa_μ in $\frac{1}{2}(g_\mu - 2)$ [25]

Scenario	$m_{1/2}$/GeV	m_0/GeV	$\tan\beta$	sgn(μ)	$\delta a_\mu/10^{-10}$
A	600	140	5	+	2.8
B	250	100	10	+	28
C	400	90	10	+	13
D	525	125	10	−	−7.4
E	300	1500	10	+	1.7
F	1000	3450	10	+	0.29
G	375	120	20	+	27
H	1500	419	20	+	1.7
I	350	180	35	+	45
J	750	300	35	+	11
K	1150	1000	35	−	−3.3
L	450	350	50	+	31
M	1900	1500	50	+	2.1

and, with (36), the relation [26]

$$\frac{\mathrm{Br}\,(l_i \to l_j\gamma)}{|\delta a_\mu|^2} \simeq \frac{\alpha}{\Gamma_i}\frac{m_{l_i}^3}{m_\mu^2}\left|\frac{A_{\rm R}^{ij}}{A_{\rm L}^{22} + A_{\rm R}^{22}}\right|^2, \quad (46)$$

where Γ_i denotes the total decay width of lepton l_i and $A_{\rm R}^{ij} \gg A_{\rm L}^{ij}$ has been used. It will be shown later that this ratio varies less with the SUSY parameters and thus provides a less model-dependent test of LFV than $\mathrm{Br}\,(l_i \to l_j\gamma)$ alone.

4 Input parameters

4.1 mSUGRA benchmark scenarios

In this paper we focus on the mSUGRA benchmark scenarios proposed in [25]. The theoretical framework of these scenarios is the constrained MSSM with universal soft supersymmetry breaking masses and R-parity conservation. Sparticle spectra corresponding to these scenarios are consistent with all experimental and cosmological constraints, in particular with

(1) direct sparticle searches;
(2) $b \to s\gamma$;
(3) cosmological relic density, with the lightest neutralino as lightest SUSY particle and dark matter candidate;
(4) Higgs searches.

This class of models involves five free parameters: the universal gaugino mass $m_{1/2}$ and the universal scalar mass m_0 at the GUT scale, the ratio $\tan\beta$ of the Higgs vacuum expectation values, the sign of the Higgs mixing parameter μ and the universal trilinear coupling parameter A_0. The values of these parameters for the benchmark scenarios are listed in Table 1. A_0 is set to zero in all scenarios. Further details can be found in [25].

Also given in Table 1 is the corresponding shift in the muon anomalous magnetic moment. The current $1.6\,\sigma$ discrepancy between the measurement of $\frac{1}{2}(g_\mu - 2)$ and the standard model prediction [32] amounts to

$$\delta a_\mu = (25 \pm 16) \cdot 10^{-10}. \tag{47}$$

Scenarios with relatively light sparticle masses below 500 GeV (e.g. B, C, G, L) are in better agreement with the above value of δa_μ than scenarios with heavier sparticles (e.g. E, F, H, M). Moreover, (47) favors a positive sign for μ.

4.2 Neutrino data

Solar and atmospheric neutrino experiments provide clear evidence for neutrino oscillations. The favored interpretation of the experimental results on solar neutrinos suggests $\nu_e \to \nu_{\mu,\tau}$ oscillations driven by the mass squared difference $\Delta m^2_{12} = m^2_2 - m^2_1$ in the range of the LMA solution, while the results on atmospheric neutrinos are interpreted by $\nu_\mu \to \nu_\tau$ oscillations driven by $\Delta m^2_{23} = m^2_3 - m^2_2$ in the case of three active neutrinos. For the present analysis, we use the global fits in a three-neutrino framework performed in [33]. In [34] it has been pointed out that the inclusion of the SNO result in a two-neutrino analysis of the solar neutrinos implies only minor changes.

We also consider the improvement in our knowledge of the neutrino sector expected from future neutrino experiments and discuss the consequences of these future accomplishments for the tests of the Majorana scale $M_{\rm R}$ considered in this paper. We always assume the present best fit values of the neutrino parameters to remain unchanged. The future improvements in the experimental errors of these parameters anticipated for a perspective view are summarized below together with other relevant expectations:

(1) Δm^2_{12} *and* $\sin^2 2\theta_{12}$: The long-baseline reactor experiment KAMLAND is designed to test the LMA MSW solution of the solar neutrino problem. Data taking is expected to start in 2002 and the solar neutrino parameters will be determined with an accuracy of $\delta(\Delta m^2_{12})/\Delta m^2_{12} = 10\%$ and $\delta(\sin^2 2\theta_{12}) = \pm 0.1$ within three years of measurement [35].

(2) Δm^2_{23} *and* $\sin^2 2\theta_{23}$: The atmospheric oscillation parameters will be determined by the long-baseline accelerator experiment MINOS with an accuracy of $\delta(\Delta m^2_{23})/\Delta m^2_{23} = 30\%$ and $\delta(\sin^2 2\theta_{23}) = \pm 0.1$ [36].

(3) $\sin^2 2\theta_{13}$: The CHOOZ reactor experiment restricts the angle θ_{13} to $\sin^2 2\theta_{13} < 0.1$ [37]. The long baseline experiment MINOS [36] can probe the range $\sin^2 2\theta_{13} \gtrsim 0.02$–$0.05$. A future superbeam, a neutrino factory [38] or the analysis of the neutrino energy spectra of a future galactic supernova [39] may provide a sensitivity at the level of a few times 10^{-3} to 10^{-4}. To explore the potential of future neutrino studies we take $\delta(\sin^2 2\theta_{13}) = 3 \cdot 10^{-3}$.

(4) *The neutrino mass spectra*: The inverse hierarchical spectrum with two heavy and a single light state is disfavored according to a recent analysis [40] of the neutrino spectrum from supernova SN1987A, unless the mixing angle θ_{13} is large (compare, however, [41]). We therefore restrict our analysis to the direct (normal) hierarchy. LFV rates for inverse hierarchical schemes lie in the intermediate range between the extreme cases we discuss, Br(degenerate) $\ll$ Br(inverse) $<$ Br(hierarchy), as pointed out in [24].

(5) *The Dirac CP phase* φ: Even at a neutrino factory, one will only be able to distinguish $\varphi = 0$ from $\pi/2$ if $\Delta m^2_{12} > 10^{-5}$ eV^2. For this reason we vary φ in the full range $0 < \varphi < 2\pi$ [42].

(6) *The neutrino mass scale*: While neutrino oscillation experiments provide information on the neutrino mass squared differences Δm^2_{ij}, the absolute scale of the neutrino masses is not known so far. Upper bounds can be obtained from the neutrino hot dark matter contribution to the cosmological large scale structure evolution and the cosmic microwave background, from the interpretation of the extreme energy cosmic rays in the Z-burst model, tritium beta decay experiments, and neutrinoless double beta decay experiments [43]. A next generation double beta decay experiment like GENIUSI, MAJORANA, EXO, XMASS or MOON will test the quantity $m_{ee} = |\sum_i V^2_{1i} \mathrm{e}^{\mathrm{i}2\phi_i} m_i|$ down to 10^{-2} eV. Since $V^2_{13} = \sin^2 2\theta_{13}/4 < 0.025$, the contribution of m_3 drops out and a bound $m_{ee} < 10^{-2}$ eV will imply $m_1 < 10^{-2}\,\mathrm{eV}/\cos 2\theta_{12}$. If one further assumes that KAMLAND measures $\sin^2 2\theta_{12}$ with $\delta(\sin^2 2\theta_{12}) = \pm 0.1$, one obtains the bound $m_1 < 3 \cdot 10^{-2}$ eV. On the other hand, a large mass m_1 could be tested by future tritium beta decay projects. A positive signal at the final sensitivity of the KATRIN experiment would imply $m_1 = 0.3 \pm 0.1$ eV [44]. Such a value would be compatible with the recent evidence claim for neutrinoless double beta decay [45].

For the present purposes, typical hierarchical and degenerate neutrino mass spectra are parametrized as follows:

(1) hierarchical $\nu_{\rm L}$ and degenerate $\nu_{\rm R}$:

$$m_1 \approx 0, \quad m_2 \approx \sqrt{\Delta m^2_{12}}, \quad m_3 \approx \sqrt{\Delta m^2_{23}}, \tag{48}$$

$$M_1 = M_2 = M_3 = M_{\rm R}. \tag{49}$$

(2) quasi-degenerate $\nu_{\rm L}$ and degenerate $\nu_{\rm R}$ [24]:

$$m_1, \quad m_2 \approx m_1 + \frac{1}{2m_1}\Delta m^2_{12},$$

$$m_3 \approx m_1 + \frac{1}{2m_1}\Delta m^2_{23}, \tag{50}$$

$$M_1 = M_2 = M_3 = M_{\rm R}, \tag{51}$$

where $m_1 \gg \sqrt{\Delta m^2_{23}} \gg \sqrt{\Delta m^2_{12}}$.

The product of Yukawa couplings $Y^\dagger_\nu Y_\nu$ appearing in the renormalization group corrections to the left-handed slepton mass matrix (27) can then be approximated by

$$\text{(a)}\ \left(Y^\dagger_\nu Y_\nu\right)_{ab} \approx \frac{M_{\rm R}}{v^2 \sin^2\beta}\sqrt{\Delta m^2_{23}}$$

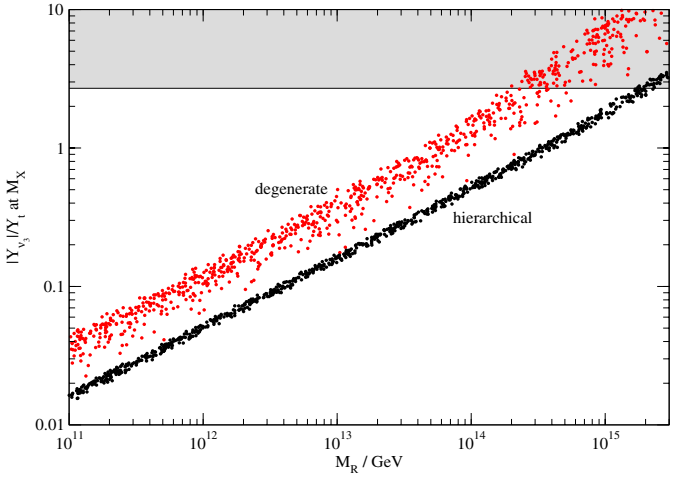

Fig. 2. Largest Yukawa coupling $|Y_{\nu_3}|$ normalized to the top Yukawa coupling Y_t at M_X for hierarchical and degenerate neutrino spectra ($\tan\beta = 30$). The shaded area is excluded by the constraint $\frac{|Y_{\nu_3}|^2}{4\pi} < 0.3$

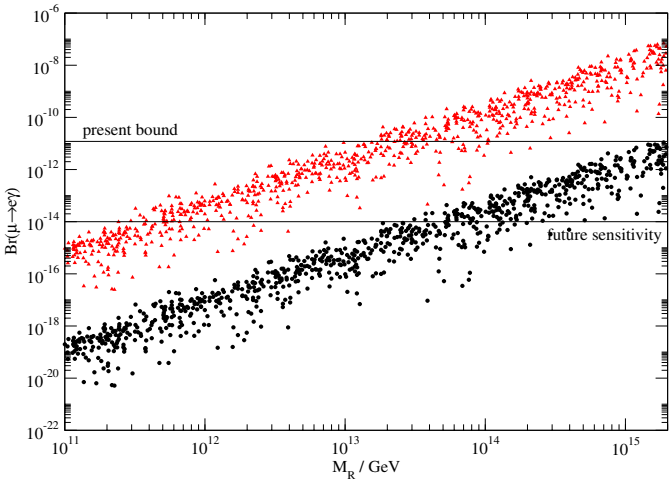

Fig. 3. Branching ratio of $\mu \to e\gamma$ for hierarchical neutrinos and uncertainties of future neutrino experiments in the mSUGRA scenarios leading to the largest (L, upper) and the smallest (H, lower) LFV rates

Table 2. 90% CL fits of neutrino parameters characterizing the present and future uncertainties. The range of the neutrino mass scale m_1 refers to a hierarchical (degenerate) spectrum

Parameter	Best fit value	Present	Future
$\tan^2\theta_{23}$	1.40	$^{+1.64}_{-1.01}$	$^{+1.37}_{-0.66}$
$\tan^2\theta_{13}$	0.005	$^{+0.050}_{-0.005}$	$^{+0.001}_{-0.005}$
$\tan^2\theta_{12}$	0.36	$^{+0.65}_{-0.16}$	$^{+0.35}_{-0.16}$
$\Delta m^2_{12}/10^{-5}\,\mathrm{eV}^2$	3.30	$^{+66.7}_{-2.3}$	$^{+0.3}_{-0.3}$
$\Delta m^2_{23}/10^{-3}\,\mathrm{eV}^2$	3.10	$^{+3.0}_{-1.7}$	$^{+1.0}_{-1.0}$
φ/rad	0 to 2π		
m_1/eV	0 to 0.03 ($0.3^{+0.11}_{-0.16}$)		

$$\times \left(\sqrt{\frac{\Delta m^2_{12}}{\Delta m^2_{23}}} V_{a2} V^*_{b2} + V_{a3} V^*_{b3} \right), \tag{52}$$

$$\text{(b)}\ \left(Y^\dagger_\nu Y_\nu\right)_{ab} \approx \frac{M_\mathrm{R}}{v^2 \sin^2\beta} \tag{53}$$

$$\times \left(m_1 \delta_{ab} + \frac{\Delta m^2_{23}}{2 m_1} \left(\frac{\Delta m^2_{12}}{\Delta m^2_{23}} V_{a2} V^*_{b2} + V_{a3} V^*_{b3} \right) \right).$$

In both cases the largest branching ratio for $l_i \to l_j\gamma$ is expected in the channel $\tau \to \mu\gamma$ because of $|V_{33}V^*_{23}| = |V_{32}V^*_{22}|$ and $\Delta m^2_{23} \gg \Delta m^2_{12}$. The decays $\mu \to e\gamma$ and $\tau \to e\gamma$ are suppressed by the smallness of Δm^2_{12} and V_{13}. In the case (b), there is an additional suppression by $\sqrt{\Delta m^2_{23}}/m_1$ or $\sqrt{\Delta m^2_{12}}/m_1$ relative to the case (a).

In the following analysis, the neutrino parameters are varied in the ranges specified in Table 2, characterizing the present knowledge and future prospects.

Note that all parameters are varied simultaneously. The Majorana mass scale M_R is treated as a free parameter. This contrasts with other approaches [19,20] where Yukawa coupling unification

$$|Y_{\nu_3}| = Y_t \text{ at } M_X \tag{54}$$

is assumed, $|Y_{\nu_3}|^2$ being the largest eigenvalue of $Y^\dagger_\nu Y_\nu$. Figure 2 shows the normalized Yukawa coupling $|Y_{\nu_3}|/Y_t$ at M_X as a function of the Majorana mass M_R. One can see that the assumption (54) would fix the Majorana mass scale to $M_\mathrm{R} \approx 4 \cdot 10^{14}$ GeV for hierarchical neutrinos and to $M_\mathrm{R} \approx 7 \cdot 10^{13}$ GeV in the degenerate case.

Figure 2 also shows that for large values of M_R, the Yukawa coupling $|Y_{\nu_3}|$ eventually gets too strong for perturbation theory to be valid. Therefore, we restrict $|Y_{\nu_3}|$ to values $\frac{|Y_{\nu_3}|^2}{4\pi} < 0.3$, which implies the consistency limits $M_\mathrm{R} < 2 \cdot 10^{15}$ GeV in the hierarchical and $M_\mathrm{R} < 3 \cdot 10^{14}$ GeV in the degenerate case. It should be stressed in this context, that since the negative mass shift δm^2_L given in (27) is driven by the neutrino Yukawa couplings, the slepton masses decrease with increasing M_R. We have checked that in the perturbative region of Y_{ν_3} defined above, the slepton masses do not violate existing lower mass bounds, in particular the LEP bound $m_{\tilde{\tau}_1} > 81$ GeV [8].

5 Numerical results

The dependence of $\mathrm{Br}(l_i \to l_j\gamma)$ on the right-handed Majorana mass scale M_R is displayed in Figs. 3, 4 and 5 for those two mSUGRA scenarios listed in Table 1 which lead to the largest and smallest branching ratios. The sensitivity on M_R for all benchmark mSUGRA scenarios defined in Table 1 is summarized in Table 3. The present bounds on $\mathrm{Br}(\tau \to e\gamma)$ and $\mathrm{Br}(\tau \to \mu\gamma)$ set relatively weak constraints on M_R and are therefore not included in Table 3. For each scenario, the neutrino input is varied in the ranges allowed by present and/or future experiments.

Comparing Figs. 3 and 4 with Fig. 5, one can see that $\mathrm{Br}(\mu \to e\gamma)$ is more strongly affected by the uncertainties in the neutrino parameters than $\mathrm{Br}(\tau \to \mu\gamma)$. This finding can be understood qualitatively from (52) and (53),

Table 3. Ranges of values for M_R for the given branching ratios in the case of hierarchical or degenerate neutrino spectra with present or future uncertainties of neutrino parameters. With "–" we denote that the sensitivity is too low

Scenario	$\mathrm{Br}(\mu \to e\gamma) = 1.2 \cdot 10^{-11}$	$\mathrm{Br}(\mu \to e\gamma) = 10^{-14}$		$\mathrm{Br}(\tau \to \mu\gamma) = 10^{-9}$
	$M_R/10^{14}$ GeV	$M_R/10^{14}$ GeV		$M_R/10^{14}$ GeV
	present/hier.	future/hier.	future/deg.	future/hier.
A	[4, 20]	[0.2, 4]	[0.9, 3]	–
B	[0.1, 20]	[0.006, 0.4]	[0.02, 2]	[1, 2]
C	[0.6, 20]	[0.04, 0.8]	[0.2, 2]	[9, 11]
D	[2, 20]	[0.07, 2]	[0.2, 2]	[15, 19]
E	[0.3, 20]	[0.02, 0.8]	[0.1, 2]	[4, 5]
F	[3, 20]	[0.2, 2]	[0.6, 2]	–
G	[0.2, 20]	[0.01, 0.4]	[0.1, 2]	[2, 3]
H	[4, 20]	[0.3, 4]	[1, 3]	–
I	[0.04, 5]	[0.003, 0.04]	[0.02, 1]	[0.3, 0.6]
J	[0.3, 20]	[0.02, 0.8]	[0.1, 2]	[3, 4]
K	[0.5, 20]	[0.03, 0.8]	[0.2, 2]	[4, 7]
L	[0.04, 5]	[0.003, 0.04]	[0.02, 0.6]	[0.2, 0.5]
M	[0.6, 20]	[0.06, 0.8]	[0.2, 2]	[6, 9]

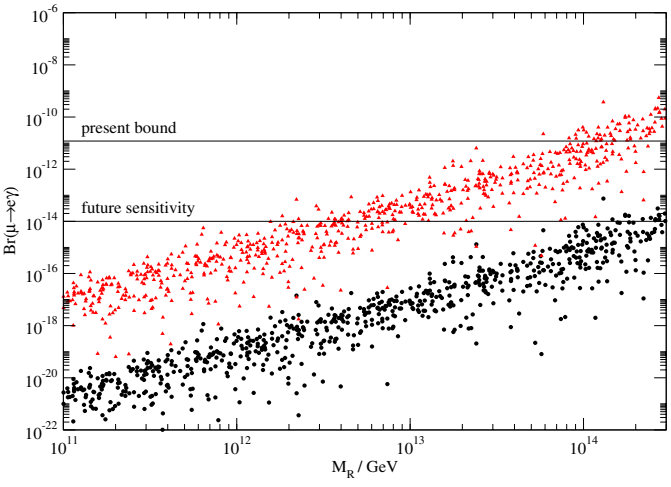

Fig. 4. Branching ratio of $\mu \to e\gamma$ for degenerate neutrinos and uncertainties of future neutrino experiments in the mSUGRA scenarios leading to the largest (L, upper) and the smallest (H, lower) LFV rates

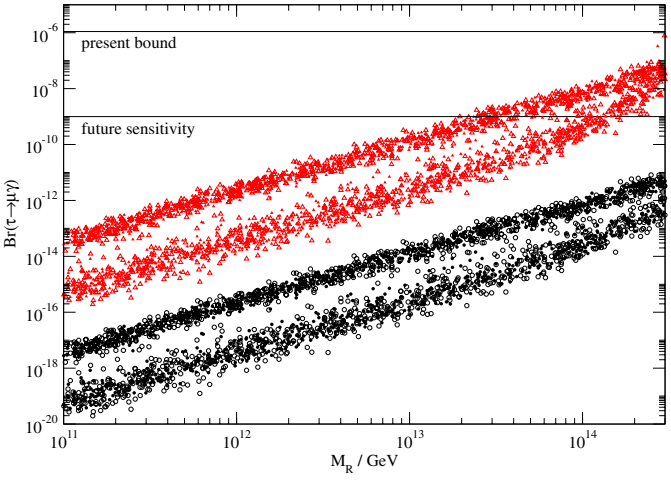

Fig. 5. Branching ratio of $\tau \to \mu\gamma$ for hierarchical (upper) and degenerate (lower) neutrino masses in the mSUGRA scenarios leading to the largest (L, triangles) and the smallest (H, circles) LFV rates. Open and filled symbols refer to neutrino measurements with present and future uncertainties, respectively

where one sees that $\tau \to \mu\gamma$ mainly depends on the large angle θ_{23} while $\mu \to e\gamma$ involves the small quantities θ_{13} and Δm^2_{12}. The difference in the scatter range of the predictions for $\tau \to \mu\gamma$ and $\mu \to e\gamma$ thus reflects the different relative error of the quantities θ_{23}, θ_{13} and Δm^2_{12} and also the complete lack of knowledge on φ (see Table 2). Furthermore Figs. 3, 4 and 5 and Table 3 show that the experimental prospects favor the channel $\mu \to e\gamma$ over $\tau \to \mu\gamma$ for testing small values of M_R. Larger values of M_R would be probed more accurately in $\tau \to \mu\gamma$.

We also find that for fixed M_R the branching ratios for $l_i \to l_j\gamma$ depend strongly on the particular mSUGRA scenario.

The strongest bounds on M_R are obtained in scenario L due to very large $\tan\beta$ and small sparticle masses, whereas scenario H with large gaugino masses yields the weakest bounds.

In summary, we find for hierarchical neutrino spectra that a future measurement of $\mathrm{Br}(\tau \to \mu\gamma) \approx 10^{-9}$ would typically determine M_R up to a factor of 2 given the uncertainties in the neutrino parameters. On the other hand, a measurement of $\mathrm{Br}(\mu \to e\gamma) \approx 10^{-14}$ would determine the right-handed scale only up to a factor of 10–100, even if the SUSY parameters would be known. Finally, assum-

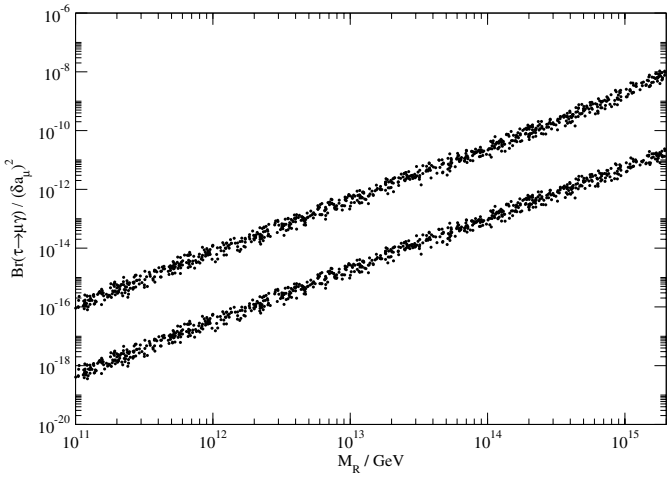

Fig. 6. Ratio $\mathrm{Br}(\tau \to \mu\gamma)/(\delta a_\mu)^2$ for hierarchical neutrinos and uncertainties of future neutrino experiments. Shown are the expectations for the mSUGRA scenarios F (upper) and C (lower) which embrace the predictions for all other benchmark scenarios of Table 1

ing an exactly massless lightest neutrino (as in previous works), the upper bounds on M_R improve by a factor of up to 10. For degenerate neutrinos and $M_\mathrm{R} < 10^{14}\,\mathrm{GeV}$, $\mathrm{Br}(l_i \to l_j\gamma)$ is suppressed by roughly two orders of magnitude as compared to the case of hierarchical neutrino spectra, but exhibit a similar dependence on M_R. This can be seen by comparing Figs. 3 and 4. However, for $M_\mathrm{R} > 10^{14}\,\mathrm{GeV}$, the neutrino Yukawa couplings increase more strongly for degenerate than for hierarchical neutrinos, as illustrated in Fig. 2. Hence for sufficiently large M_R, the branching ratios for hierarchical and degenerate neutrinos become comparable. This behavior is particularly pronounced for $\mathrm{Br}(\tau \to \mu\gamma)$ as indicated in Fig. 5, because of the enhanced loop contribution from the lightest stau.

6 Conclusions

Future experiments searching for lepton-flavor violating rare processes can test the Majorana mass scale M_R of right-handed neutrinos in the see-saw mechanism. We have systematically and comprehensively studied the sensitivity of $\mathrm{Br}(l_i \to l_j\gamma)$ on M_R in mSUGRA benchmark scenarios designed for future collider studies taking into account the uncertainties of present and future neutrino measurements. We have assumed degenerate Majorana masses for the right-handed neutrinos and a normal neutrino mass hierarchy, and have considered hierarchical and degenerate neutrino spectra.

For hierarchical neutrinos the measurement of $\mathrm{Br}(\mu \to e\gamma) \approx 10^{-14}$ would probe M_R in the range $5 \cdot 10^{12}\,\mathrm{GeV}$ to $5 \cdot 10^{14}\,\mathrm{GeV}$, depending on the mSUGRA scenario. On the other hand, a future measurement of $\mathrm{Br}(\tau \to \mu\gamma)$ at a level of 10^{-9} will determine M_R in the range larger than $5{\cdot}10^{13}\,\mathrm{GeV}$ with an accuracy of a factor of 2 for a given scenario. In the case of degenerate neutrino masses the upper bound on M_R which can be derived from $\mathrm{Br}(\mu \to e\gamma) < 10^{-14}$ is $(1\text{–}3) \cdot 10^{14}\,\mathrm{GeV}$, independently of the mSUGRA scenario. Unification of the top Yukawa coupling and the Yukawa coupling of the heaviest neutrino at M_X would fix M_R to $M_\mathrm{R} \approx 4 \cdot 10^{14}\,\mathrm{GeV}$ and $M_\mathrm{R} \approx 7 \cdot 10^{13}\,\mathrm{GeV}$ for hierarchical and degenerate neutrinos, respectively. This proposition can thus be tested in the future.

Planned measurements of $\mu \to 3e$ are not expected to improve the bounds on M_R. On the other hand, a future measurement of $R\,(\mu^-\mathrm{Ti} \to e^-\mathrm{Ti}) \approx 10^{-18}$ is found to be more sensitive to M_R by a factor of about 2 than $\mathrm{Br}\,(\mu \to e\gamma) \approx 10^{-15}$.

The correlation between the SUSY contribution δa_μ to $g_\mu - 2$ and $\mathrm{Br}(l_i \to l_j\gamma)$ can be used to reduce the mSUGRA scenario dependence of the above tests. Comparing the ratio $\mathrm{Br}(\tau \to \mu\gamma)/(\delta a_\mu)^2$ in Fig. 6 with the branching ratio for $\tau \to \mu\gamma$ shown in Fig. 5, one can see that for fixed M_R and different mSUGRA scenarios the ratio varies by two orders of magnitude less than the value of $\mathrm{Br}(\tau \to \mu\gamma)$ itself.

Acknowledgements. We thank M. C. Gonzalez-Garcia, J. Hisano, A. Ibarra and A. Parkhomenko for useful discussions. This work was supported by the Bundesministerium für Bildung und Forschung (BMBF, Bonn, Germany) under the contract number 05HT1WWA2.

References

1. Q.R. Ahmad et al. [SNO Collaboration], Phys. Rev. Lett. **87**, 071301 (2001) [nucl-ex/0106015]
2. Y. Fukuda et al. [Super-Kamiokande Collaboration], Phys. Rev. Lett. **81**, 1562 (1998) [hep-ex/9807003]
3. M. Gell-Mann, P. Ramond, R. Slansky, Proceedings of the Supergravity Stony Brook Workshop, New York 1979, edited by P. Van Nieuwenhuizen, D. Freedman; T. Yanagida, Proceedings of the Workshop on Unified Theories and Baryon Number in the Universe, Tsukuba, Japan 1979, edited by A. Sawada, A. Sugamoto; R.N. Mohapatra, G. Senjanovic, Phys. Rev. Lett. **44**, 912 (1980); Erratum, Phys. Rev. D **23**, 165 (1993)
4. S.T. Petcov, Sov. J. Nucl. Phys. **25**, 340 (1977) [Yad. Fiz. **25**, 641 (1977); Erratum, **25**, 698 (1977); Erratum, **25**, 1336 (1977)]; S.M. Bilenkii, S.T. Petcov, B. Pontecorvo, Phys. Lett. B **67**, 309 (1977)
5. J. Hisano, T. Moroi, K. Tobe, M. Yamaguchi, Phys. Rev. D **53**, 2442 (1996) [hep-ph/9510309]
6. M.L. Brooks et al. [MEGA Collaboration], Phys. Rev. Lett. **83**, 1521 (1999) [hep-ex/9905013]
7. L.M. Barkov et al., Research Proposal R-99-05.1 for an experiment at PSI (1999)
8. D.E. Groom et al. [Particle Data Group Collaboration], Eur. Phys. J. C **15**, 1 (2000) and 2001 partial update for edition 2002
9. S. Ahmed et al. [CLEO Collaboration], Phys. Rev. D **61**, 071101 (2000) [hep-ex/9910060]
10. L. Serin, R. Stroynowski, ATLAS Internal Note (1997); D. Denegri, private communication; T. Ohshima, talk at the 3rd Workshop on Neutrino Oscillations and their Origin (NOON2001), 2001, ICRR, University of Tokyo, Kashiwa, Japan, to appear in the Proceedings

11. U. Bellgardt et al. [SINDRUM Collaboration], Nucl. Phys. B **299**, 1 (1988)
12. P. Wintz, Proceedings of the First International Symposium on Lepton and Baryon Number Violation, edited by H.V. Klapdor–Kleingrothaus, I.V. Krivosheina (Institute of Physics, Bristol 1998), p. 534
13. SINDRUM II collaboration, Research Proposal R-89-06 for an experiment at PSI (1989)
14. M. Bachmann et al. [MECO collaboration], Research Proposal E940 for an experiment at BNL (1997)
15. W. Ootani, talk at the 3rd Workshop on Neutrino Oscillations and their Origin (NOON2001), 2001, ICRR, University of Tokyo, Kashiwa, Japan, to appear in the Proceedings
16. J. Aysto et al. [hep-ph/0109217], Report of the Stopped Muons Working Group for the ECFA-CERN study on Neutrino Factory & Muon Storage Rings at CERN
17. K. Yoshimura, talk at the 3rd Workshop on Neutrino Oscillations and their Origin (NOON2001), 2001, ICRR, University of Tokyo, Kashiwa, Japan, to appear in the Proceedings
18. Y. Kuno, Y. Okada, Rev. Mod. Phys. **73**, 151 (2001) [hep-ph/9909265]
19. J. Hisano, D. Nomura, Phys. Rev. D **59**, 116005 (1999) [hep-ph/9810479]
20. J.A. Casas, A. Ibarra, Nucl. Phys. B **618**, 171 (2001) [hep-ph/0103065]
21. R. Barbieri, L. Hall, A. Strumia, Nucl. Phys. B **445**, 219 (1995); G.K. Leontaris, N.D. Tracas, Phys. Lett. B **431**, 90 (1998); K.S. Babu, B. Dutta, R.N. Mohapatra, Phys. Lett. B **458**, 93 (1999) [hep-ph/9904366]; W. Buchmuller, D. Delepine, F. Vissani, Phys. Lett. B **459**, 171 (1999); M.E. Gomez, G.K. Leontaris, S. Lola, J.D. Vergados, Phys. Rev. D **59**, 116009 (1999); S.F. King, M. Oliveira, Phys. Rev. D **60**, 035003 (1999); W. Buchmuller, D. Delepine, L.T. Handoko, Nucl. Phys. B **576**, 445 (2000); J. Ellis, M.E. Gomez, G.K. Leontaris, S. Lola, D.V. Nanopoulos, Eur. Phys. J. C **14**, 319 (2000); J.L. Feng, Y. Nir, Y. Shadmi, Phys. Rev. D **61**, 113005 (2000); J. Sato, K. Tobe, Phys. Rev. D **63**, 116010 (2001); D.F. Carvalho, M.E. Gomez, S. Khalil, JHEP **0107**, 001 (2001); J.R. Ellis, J. Hisano, M. Raidal, Y. Shimizu, hep-ph/0206110
22. J. Sato, K. Tobe, T. Yanagida, Phys. Lett. B **498**, 189 (2001); S. Davidson, A. Ibarra, JHEP **0109**, 013 (2001)
23. P. Ciafaloni, A. Romanino, A. Strumia, Nucl. Phys. B **458**, 3 (1996); J. Hisano, T. Moroi, K. Tobe, M. Yamaguchi, Phys. Lett. B **391**, 341 (1997); J. Hisano, D. Nomura, Y. Okada, Y. Shimizu, M. Tanaka, Phys. Rev. D **58**, 116010 (1998); J. Hisano, D. Nomura, T. Yanagida, Phys. Lett. B **437**, 351 (1998); S.W. Baek, N.G. Deshpande, X.G. He, P. Ko, Phys. Rev. D **64**, 055006 (2001); G. Barenboim, K. Huitu, M. Raidal, Phys. Rev. D **63**, 055006 (2001); X.J. Bi, Y.B. Dai, S. Lavignac, I. Masina, C.A. Savoy, Phys. Lett. B **520**, 269 (2001)
24. A. Kageyama, S. Kaneko, N. Shimoyama, M. Tanimoto, Phys. Rev. D **65**, 096010 (2002) [hep-ph/0112359]
25. M. Battaglia et al., Eur. Phys. J. C **22**, 535 (2001) [hep-ph/0106204]
26. D.F. Carvalho, J.R. Ellis, M.E. Gomez, S. Lola, Phys. Lett. B **515**, 323 (2001) [hep-ph/0103256]
27. J.R. Ellis, S. Lola, Phys. Lett. B **458**, 310 (1999) [hep-ph/9904279]
28. W. de Boer, Prog. Part. Nucl. Phys. **33**, 201 (1994) [hep-ph/9402266]
29. J.R. Ellis, M.E. Gomez, G.K. Leontaris, S. Lola, D.V. Nanopoulos, Eur. Phys. J. C **14**, 319 (2000) [hep-ph/9911459]
30. Y. Okada, K.I. Okumura, Y. Shimizu, Phys. Rev. D **61**, 094001 (2000) [hep-ph/9906446]
31. J.R. Ellis, J. Hisano, S. Lola, M. Raidal, Nucl. Phys. B **621**, 208 (2002) [hep-ph/0109125]
32. M. Knecht, A. Nyffeler, Phys. Rev. D **65**, 073034 (2002) [hep-ph/0111058]
33. M.C. Gonzalez-Garcia, M. Maltoni, C. Pena-Garay, J.W. Valle, Phys. Rev. D **63**, 033005 (2001) [hep-ph/0009350]
34. J.N. Bahcall, M.C. Gonzalez-Garcia, C. Pena-Garay, [hep-ph/0204314]
35. V. Barger, D. Marfatia, B.P. Wood, Phys. Lett. B **498**, 53 (2001) [hep-ph/0011251]
36. MINOS Technical Design Report, http://www.hep.anl.gov/ndk/hypertext/minos_tdr.html
37. M. Apollonio et al. [CHOOZ Collaboration], Phys. Lett. B **466**, 415 (1999) [hep-ex/9907037]
38. V. Barger, talk at Joint U.S. / Japan Workshop on New Initiatives in Muon Lepton Flavor Violation and Neutrino Oscillation with High Intense Muon and Neutrino Sources, Honolulu, Hawaii, 2000, to appear in the Proceedings [hep-ph/0102052]
39. A.S. Dighe, A.Y. Smirnov, Phys. Rev. D **62**, 033007 (2000) [hep-ph/9907423]
40. H. Minakata, H. Nunokawa, Phys. Lett. B **504**, 301 (2001); C. Lunardini, A.Y. Smirnov, Phys. Rev. D **63**, 073009 (2001)
41. V. Barger, D. Marfatia, B.P. Wood, Phys. Lett. B **532**, 19 (2002) [hep-ph/0202158]
42. J.J. Gomez-Cadenas, Nucl. Phys. Proc. Suppl. B **99**, 304 (2001) [hep-ph/0105298]
43. H. Päs, T.J. Weiler, Phys. Rev. D **63**, 113015 (2001) [hep-ph/0101091]
44. A. Osipowicz et al. [KATRIN Collaboration], hep-ex/0109033; C. Weinheimer, private communication
45. H.V. Klapdor-Kleingrothaus, A. Dietz, H.L. Harney, I.V. Krivosheina, Mod. Phys. Lett. A **16**, 2409 (2001) [hep-ph/0201231]